Surface and Wetting Properties of Diagenetic Minerals and Sedimentary Grains in Reservoir Rocks (NanoPorO)

Altermann W. (1)*, Drobek T. (1), Frei M. (1), Heckl W.M. (2), Kantioler M. (1), Phuong K.L. (1), Stark R.W. (3), Strobel J. (4), Wolkersdorfer C. (1)

(1) LMU, Geology, Sedimentology, Crystallography, wlady.altermann@iaag.geo.uni-muenchen.de, tanja.drobek@lrz.uni-muenchen.de, michaela.frei@iaag.geo.uni-muenchen.de, markus@kantioler.de, Kimphuong.Lieu@lrz.uni-muenchen.de

(2) TU Munich, TUM School of Education & Deutsches Museum München, w.heckl@deutsches-museum.de

(3) TU Darmstadt, Center of Smart Interfaces, stark@csi.tu-darmstadt.de

(4) RWE Dea, Hamburg, Joachim.Strobel@rwe.com

* Coordinator of the project

Introduction

Current secondary oil recovery measures allow for the recovery of a maximum of about 33 % of the oil in a reservoir. The remaining almost two third of the energy carrier are lost due to decreasing pressure, pore blocking, water invasion or hydrocarbon fluid adhesion to the rock. Therefore, fluids weakening the adhesion of hydrocarbons to pore walls and increasing permeability of the rock by e.g. mineral cement dissolution, are injected to the deposits in order to augment production. All such measures however, including enhanced oil recovery (EOR) methods such as the injection of supercritical CO_2 may increase the recovery factor of the original oil in place by further 10 % only. Consequently, most of the hydrocarbon wealth in oil and gas reservoirs cannot be extracted and is lost to future generations. It is thus of high importance to understand the fundamental wetting processes in the pore space, to better develop the potential of oil and gas production from reservoir rocks and to secure the fossil energy supply.

In siliciclastic oil and gas reservoir rocks, the pore space typically faces mineralogically varying sedimentary grains and various diagenetic minerals. Most common are mineral surfaces of quartz, feldspar, phyllosilicates, carbonates and iron oxides and hydroxides. This mineralogy surrounding the pore space, and the surface chemistry, topography and roughness on the micro and nano-scale rule the wetting behavior and adhesion properties of hydrocarbon fluids, water, or CO_2 to the pore walls. The dispersion, migration, adhesion and reactivity of fluids in rocks depends also on pressure and temperature conditions, nevertheless, particularly the morphology of pore walls and the pore and pore-throat shapes, have a significant impact on the behavior of the water-gas contact depth (WGC) and on the potential recovery of hydrocarbons from the given reservoir rock.

Each episode of fluid transport through the rock leaves a significant and characteristic trace in cement mineralogy, pore morphology, permeability, but often also in sediment grain or bioclast alteration. Such processes can be defined down to the nanoscale and play a crucial role in further mobility of hydrocarbons in rocks *(Hassenkam et al., 2009*). Sediment wetting varies with the alteration of the surfaces and depends on surface roughness, surface charges, and the chemical composition of the liquid phase (*Al-Futaitsi et al., 2003; Al-Futaisi and Patzek, 2004*). The interfacial tension of

the fluids strongly depends on the composition of the coexisting phases (*Sutjiadi-Sia et al., 2008*). In addition, the presence of a supercritical (sc)CO_2 phase can affect the wetting properties of the other phases due to mass exchange as a function of pressure (*Foullac et al., 200; Sutjiadi-Sia et al., 2008; Jäger and Pietsch, 2009*). It is, however, not clear how the specific conditions of the reservoir (p, T, surface chemistry and morphology) affect the interfacial tension of the relevant fluids. To understand the fundamental physico-chemistry helps to design new technologies for tertiary exploitation measures and for CO_2-storage (Carbon Capture and Storage: CCS). In this project we investigate the relationship between various minerals or grains facing the pore space, to fluids in reservoir rocks and to CO_2 and scCO_2 (*Altermann et al., 2008*). In the following we report on the geological and physical characterization of the reservoir rock under investigation and on the characterization of wetting of rough model surfaces in scCO_2.

Characterisation of the rocks and the pore space

The RWE Dea AG, Hamburg, provided cores and plugs of sandstone reservoir rocks with varying physical properties such as permeability, porosity, grain sizes and mineralogy from north German oil and gas deposits. The samples are well indurated, but still slightly friable, fine to medium grained, with sparry cements and with abundant pale and dull grains (see e.g. Fig. 1). From each sample several petrographic sections were obtained. The porosity was stained blue but no other stains (e.g. for feldspars or carbonates) were applied. In thin section, the samples may show some indistinct alternating lamination of coarser and finer grains and partly with differing cement and open pore space volume. Some samples however, exhibit very distinct lamination defined by grain size, mineralogy and porosity changes. Most sandstone samples are structurally medium mature but compositionally heterogeneous and immature. The grains are very well to well rounded, sometimes sub-rounded when finer, but appear also facetted, subrounded to poorly rounded because of dissolution under pressure, along grain to grain contacts (sutured contacts) and because of grain dissolution along boundaries during diagenesis (comp. below). The sorting of grain sizes and elongation are moderate to poor. Most grains are rather subspheroidal although distinctly

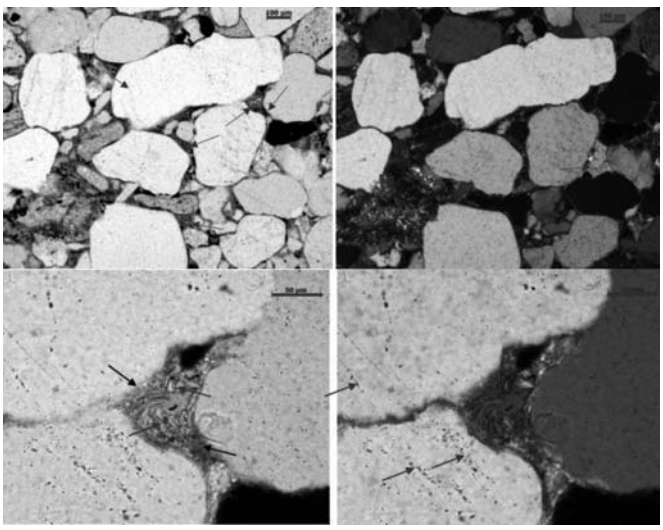

Figure 1: Grain under single (left side) and double (right side) polarised light. Scale in the upper right corners is 100µm. Chlorite is filling the pore space overgrowing hematite skins and the grains as pointed out by the arrows in picture on the left. The open pore space in the upper right corner of the upper picture pair displays haematite followed by chlorite growing tangentially into the open pore (enlargement in the lower pictures). The large elongated quartz grain in the upper part of the upper picture is syntaxially overgrown by quartz cement. The original grain boundary is pointed out by the arrow. In the upper right picture, calcite cement (right arrow) is also visible. The left arrow points to an altered feldspar with sericite inclusions. Sericite matrix can be also found between some grain boundaries. In the lower, enlarged view chlorite growing tangentially (arrows) is overgrowing haematite skins (arrows). The open pore space displays small fans of chlorite facing the open pore. Fluid inclusion trails can be seen in the quartz grains (pointed out by arrows in the lower right picture. Sutured grain contact can be recognised between the two grains on left hand side of the lower pictures.

elongated grains occur as well. The elongation seems not to depend on the grain composition. The sorting varies from laminae to laminae but is always not very high and smaller grains always are compacted between larger grains, with rare coarse sand sizes and common fine and medium grain sizes present. Rounding of grains strongly depends on the size, fine sand being significantly less rounded and less spheroidal than medium and coarse sand grains. All these properties are somewhat obliterated by widespread syntaxial quartz and albite overgrowth, which appears unambiguous only when observed under crossed polarisator.

Grain composition is of about 60 % to 70 % quartz grains. Albite, plagioclase and K-feldspar grains are also present and common. Quartzite, recrystallised chert, vein quartz and igneous rock fragments constitute less than 5 % of the grain content, the composition of the sandstones hints towards a cratonic source with mixed sedimentary and igneous rocks. This is supported by the presence of detrital phyllosilicates (muscovite and altered, greenish biotite) compacted between the quartz, feldspar and rock fragment grains. Few rounded, detrital, opaque ore grains (heavy minerals) were also found. The matrix varies between silt size detrital grains, clay minerals (primary and as alteration products of some unknown, probably volcanic and igneous rock fragment precursor), and patches and interstices with haematitic filling (possible alteration).

All samples exhibit a complicated polyphase diagenetic history. Sutured contacts and grain dissolution features evidence significant fluid movement during diagenesis. The diagenetic minerals were precipitated from migrating brians in the pore space, as synthaxial and normal quartz overgrowth cement, but also very commonly as albite cements, confirmed by EDAX analyses (see Fig. 2 and 3). Very often, the first generation of cement/matrix is that of chlorite and clay minerals and /or haematite skins sur-

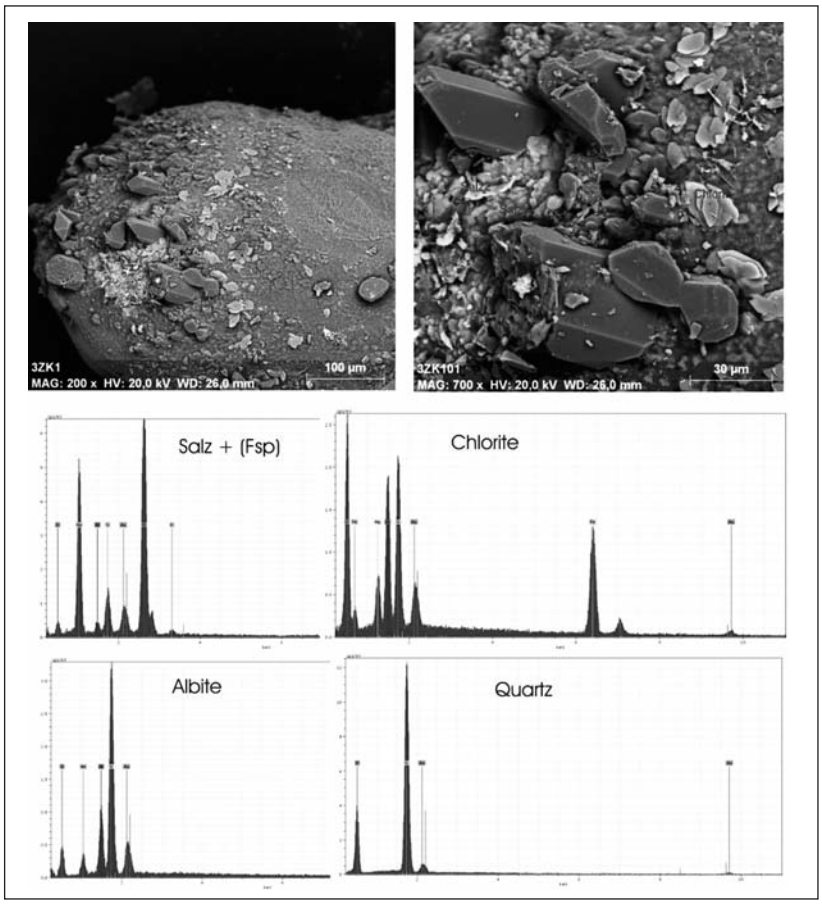

Figure 2: The left upper SEM micrograph displays an overview of the grain surface with idiomorphic minerals growing on the grain into the open pore space. The right hand image shows a close up view of this overgrowth, displaying idiomorphic mineral habitus of chlorite, quartz, albite (not well developed) and halite skin (Salz) and the respective EDX measurements. In the halite diagram (upper left) feldspar content is visible below the halite encrustation and thus Al and K peaks are visible as well.

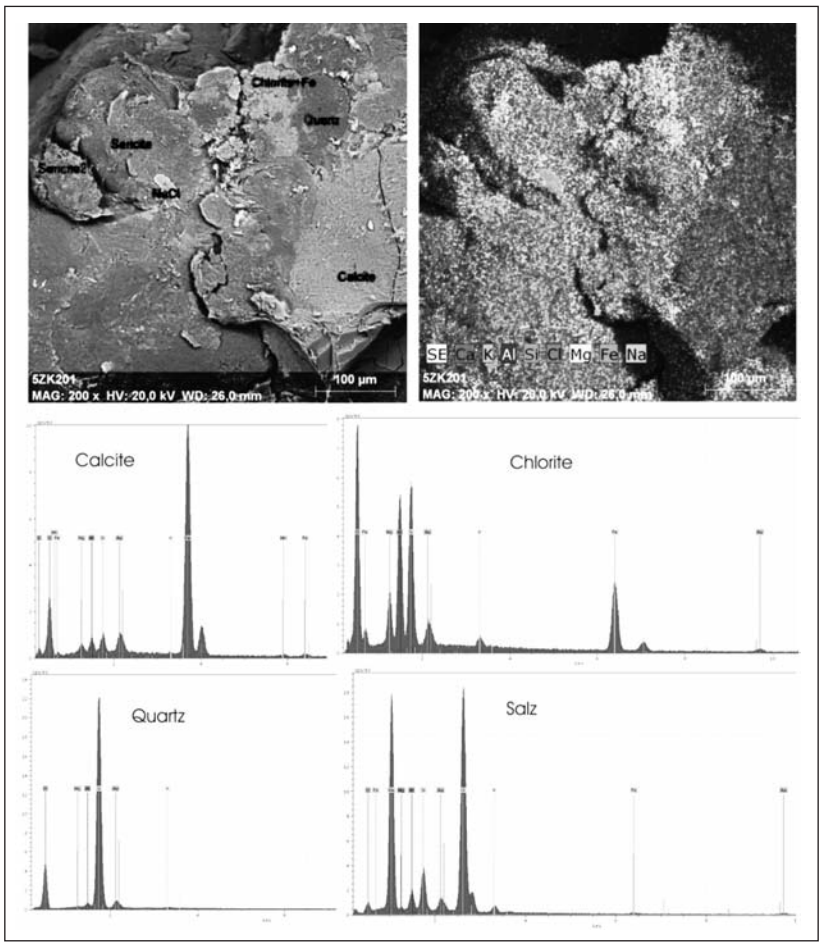

Figure 3: The left picture displays an overview of grain and cements with respective spots of EDX analysis, as shown in diagrams below. Chlorite, sericite, calcite, halite (Salz, NaCl) and quartz were found. The right hand picture displays an EDX elemental map of the view in left picture. The large area of calcite cement appears on the right side of the picture. Most of the other area is occupied by quartz cement.

rounding the grains. In a later diagenesis quartz and albite coatings were generated. Clay minerals, chlorite, haematite coats are present as the second and third cement generation as well. Partial decementation – dissolution of these neomorphic minerals, is evident in laminae, where such cements are much thinner and very irregular, leaving out abundant open pore space and by partial filling of the interstices with calcite, as most probably the latest stage of cementation. This is particularly clear where calcite is the only remaining pore filling cement and in direct contact to the detrital grains, but passing (overlapping) laterally onto quartz and albite cements. In such cases, it becomes apparent that the process was not a gradual replacement of former cements by calcite, but instead, the early cements were partly dissolved and transported aside in solution, and only subsequently, calcite was precipitated from migrating fluids. Calcite together with other cements thus, often fills resorption embayments but also dissolution pits in the grains.

SEM investigations were performed on single grains broken off from the core samples, pikked with pincers, mounted on a conventional SEM mount carrier disk with double-sided stikking tape, and coated with sputtered carbon. Elemental mapping was conducted by the EDX. In most cases cements fully cover the grains by multiple coats of various minerals. The outer most layers very often exhibit idiomorphic crystals facing the open pore space. The involved minerals are clay mineral platelets, albite twins, chlorite fans, idiomorphic, pseudohexagonal quartz needles and abundant salt (halite - NaCl) as hoppers and skins. The faces of these idiomorphic crystals are absolutely flat and smooth on sub micrometer scale. Where the coatings build a tangential skin without idiomorphic faces, the roughness is just below 1µm scale and can be well observed by the SEM. Typical crystalline surfaces with pitted regular crystallographic pattern are recognizable. As could be expected from the evaluation of the cements under optical micro-

Figure 4: The LSM and optical photographs show cements of different shape within a pore of the investigated sandstone. On the left hand side albite blades are visible. In the center of the pore needles of illite grow into the pore space on quartz overgrowth of a clastic grain. Some of the needles seem also to grow from the albite surface.

scope, only calcite does not produces idiomorphic crystals. It has been observed as broken surfaces only, because it is the latest stage of cementation usually filling the pore space as one crystal, poikilotopic infill of several neighboring pores.

AFM investigations were performed on single grains or small, cemented and bond grain groups of 2-10 grains, mounted on a small metal plate sample carrier and fixed by a commercial nail varnish. The video camera mounted on the AFM table allows for a high magnification observation of the grains (500x). It was difficult, but nevertheless possible, to relocate the same spots under the AFM and SEM. The measured surface roughness of the sample depends on the scale of observation. At all scales however, the roughness is significant and the topography as shown in the profiles in both directions, vertically and horizontally, is always steep and distinct. This provides problems as to the choice of the right AFM tip. The measurement precision achieved in vertical direction was of up to few tens of nm on ideal surfaces; surfaces of steep and high roughness however, were not possible to measure exactly.

Further roughness and topography measurements were performed by a digital laser scanning microscope (laser profilometer, LSM Keyence). The LSM delivers digitally sandwiched surface images of the sample, with high depth of focus and a quantitative topography data set in µm resolution (Fig. 4). The advantage of such measurements is the ability of the LSM to exactly resolve even very steep topography, although the resolution is by an order of magnitude lower than that of an AFM or a light interferometer. Fig. 5 shows an example where the grain surface is covered by cement and hematite. Additionally, needles (illite) grow into the pore space. Such needles can affect the fluid transport in the porous network and retain hydrocarbons. This example also shows that a microscopic inspection of the pore space is essential to identify relevant morphological features and that the complicated surface

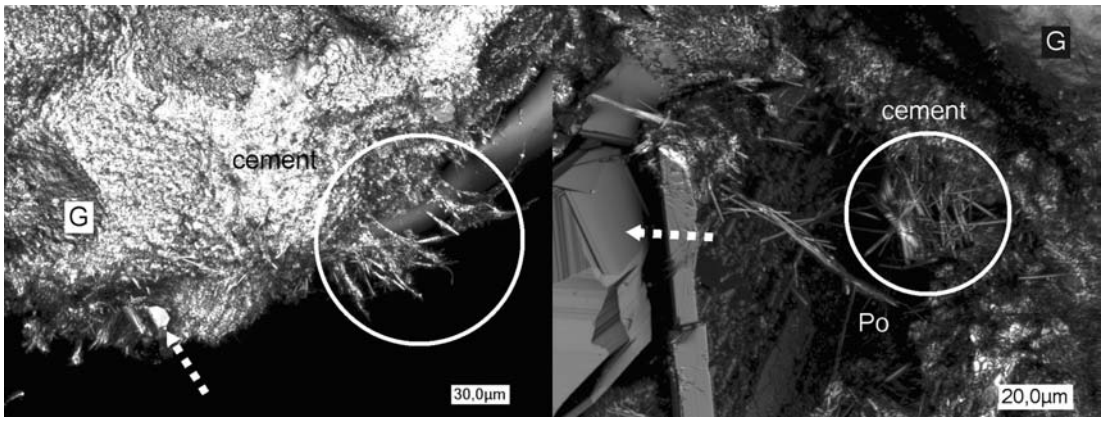

Figure 5: (left) Boundary of grain and part of grain surface (G) The grain covered by hematite skin has been stressed at the concave areas (dissolution depressions) and cement has overgrown the surface subsequently, while at the pore boundary illite needles (circle) are growing into the open pore space (Po). The sub-euhedral minerals with platy habitus are albite (dotted arrow in the right picture).

topography can not be simply described or measured by an AFM on a larger (>10 µm) scale.

As it is often difficult to identify very small grains or cements by optical microscopy, and almost impossible to identify the mineralogy by the AFM or LSM, therefore the above investigations were supported by micro-Raman spectroscopy in order to aid the mineral identification, performed mostly on thin sections and on single grain mounts. Our micro–Raman device is attached to a confocal microscope, which allows for three-dimensional imaging and for simultaneous chemical analysis. The confocal configuration leads to a small sample volume, from which Raman scattering can be recorded. Lateral and vertical cross-sections of the sample can easily be generated with high spatial resolution, whereby lateral and vertical 1-µm-thick optical slices are acquired from the surface to the maximum depth of 25 µm. The technical set up [confocal Raman microscope, alpha300 R; WITec GmbH, Ulm, Germany, frequency doubled Nd:YAG laser (532 nm, P_{max} = 22.5 mW) and a 100× objective (Nikon, NA=0.90, 0.26 mm working distance)] is described in detail in Kremer et al. (in press).

Due to the above described properties, the pore space in the investigated samples is very heterogeneous and has a wide range of mineralogical and roughness characteristics. The observed variety of the open pore morphology depends strictly on the shape of the detrital grains, on the vesicular cement minerals of tangential and needle-like habitus and on the fringing dissolution and pressure dissolution of the grains, that are mostly densely packed and grain supported. It is thus chiefly the diagenetic history and not the sedimentary history in these samples that rules the gross and nanomorphology of the pores. In order to simplify the search for a suitable target for experiments, the pores were classified according to the key mineralogy, into four main classes, each comprising several subclasses:

1) Not overgrown, rare grain surface/pore space contacts of varying mineralogy, but mainly quartz, feldspar and common volcaniclasts and heterogeneous rock fragment surfaces.
2) Quartz cement/pore space contact of botryoidal or hypidiomorphic quartz.
3) Calcite cement/pore space contact of varying shapes but mostly blocky and needle shaped or irregular, corroded calcite.
4) Heterogenous haematite, illite, chlorite albite cement/pore space contacts of differing morphologies.

Small Angle Neutron Scattering

A combination of small angle neutron scatte-

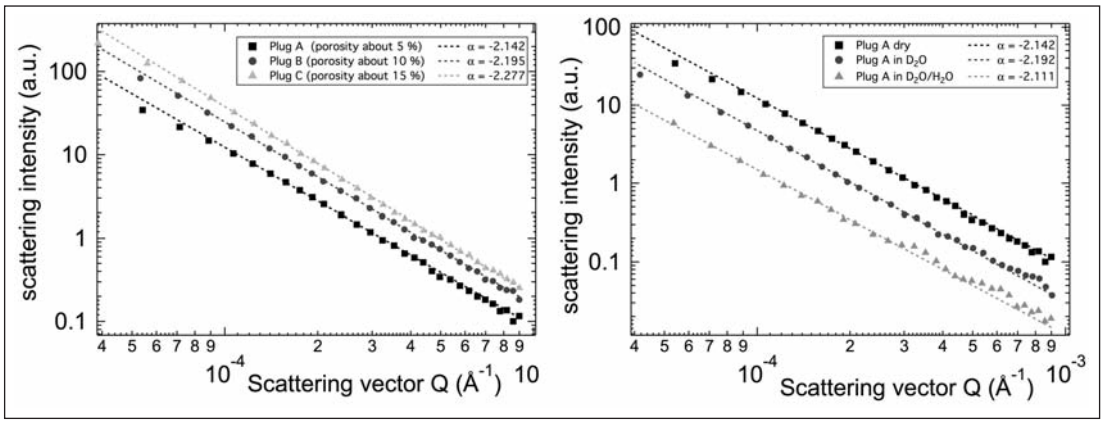

Figure 6: (left) Ultra small angle neutron scattering data of different plug samples from a quartz sandstone reservoir rock of a north German gas deposit. The intensities show a power law behaviour. With an exponent of about -2.2, indicating a mass fractal topography. (right) Filling the pores with D_2O or a contrast-matching mixture of D_2O and H_2O reduces the scattering intensity.

ring (SANS) and ultra-small angle neutron scattering (USANS) experiments on dry and partially wetted reservoir rock samples has been carried out at the Institut Laue-Langevin (ILL), in Grenoble, France in September 2010. The measurements will give insight into the interplay between texture, pore surface roughness, size distribution of the cement overgrowth and the distribution of connate water in the pore network.

Molecular scale interactions between fluids and mineral surfaces have a crucial impact on pore volume estimation, on the understanding of hydrocarbon migration, and on the possible degree of exploitation. These interactions also influence the assessment of CO_2 storage capacity and retention mechanisms or of the potential of geothermal energy generation in aquifers (*Pruess and Azaroual, 2006; Pruess, 2008*). The study aims to reveal nanoscale processes in the pore- space of sedimentary rocks in order to explain the migration processes and the permeability for fluids, gas and supercritical CO_2 within sedimentary rocks.

For reservoir rocks it is important to study the intact porous network within a representatively large volume of a bulk sample. Sandstones, mainly composed of quartz grains, show diverse heterogeneous textures, accessory minerals, and varying grain sizes of 5 ~ 100 m. Notably, capillary bound water in the pore system appears to reduce the permeability. The penetration power of neutrons allows to investigate the porosity of such bulk samples with SANS. This method is more powerful in combination with ultra small angle neutron scattering (USANS) for the study of the microstructure of rocks over a large range of scales (*Radlinski, 2006; Triolo et al., 2000; Sen et al., 2002*). The fractal dimension derived from the SANS/USANS data can be correlated to microscopy data (*Wong and Howard, 1986; Wong and Bray, 1988; Radlinski et al., 2004; Anovitz et al., 2009*) and used as a parameter for the correlation of porosity and permeability of rocks in conjunction with their pore topology (*Pape et al., 1999; Pape and Clauser, 2000*). At the beam lines D11 and S18 at ILL SANS and USANS experiments were carried out on the same set of samples. Pore filling and capillary condensation of fluids in porous media was observed with SANS and USANS by using contrast-matching H_2O/D_2O mixtures (*Broseta et al., 2001; Erko et al., 2010*).

In Figure 6 (left) data measured on sandstone reservoir rock samples of different depth and different porosity are shown. The scattering intensities follow a power law behavior, which is typical for porous rocks with an exponent of about -2.2, which corresponds to a mass fractal topography of the pore space with a

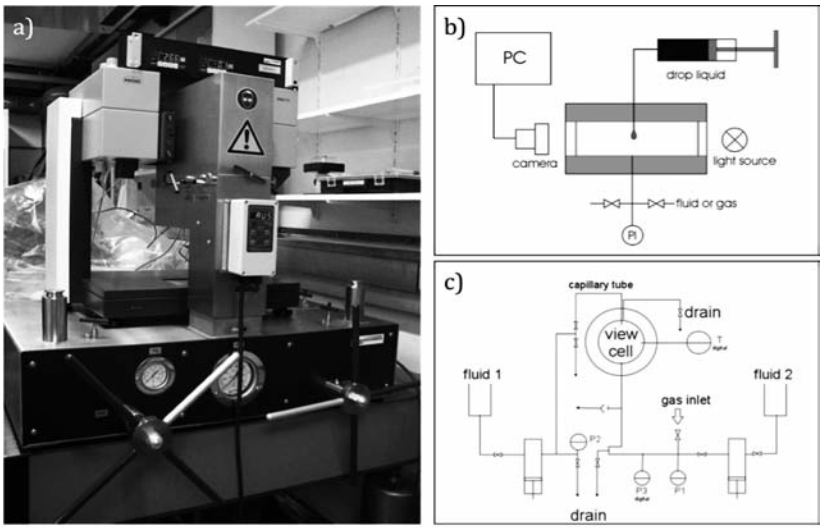

Figure 7: High Pressure View cell (Krüss GmbH, Hamburg, Eurotechnica, Bargteheide). The cylindrical cell has two optical windows. A drop can be placed on the sample surface through a capillary. The cell can be filled with two different gaseous or fluid media. Liquid CO_2 can be pressurized up to 69 MPa and heated to 180 °C. The cell is equipped with a contact angle measurement system.

dimension of 2.2. Filling the pores with D_2O or a mixture of D_2O and H_2O, contrast-matching to quartz and feldspar, massively reduced the scattering intensity. The remaining scattering contrast is mainly caused by the surfaces of calcite cement, heavy minerals and other minor constituents of the rock.

Wettability of rough surfaces at reservoir conditions

The wettability of the reservoir rock has a large influence on the productivity of a hydrocarbon reservoir. In oil fields, depending on the type of wetting characteristics of the rocks, different technologies for developing a field are necessary. One of the most prominent effects of the micro- and nano-morphology on wetting is the super-hydrophobicity, better known as the »lotus effect« on glass or ceramics (*Barthlott and Neinhuis, 1997; Neinhuis and Barthlott, 1997; Spori et al., 2008*). The lotus effect is caused by an only partial wetting of the rough surface profile by the liquid phase in the so-called Cassie-Baxter regime (*Wenzel, 1936; Cassie and Baxter, 1944*). So far, however, it is not clear how the presence of a supercritical phase and mass transport between the wetting and the supercritical phase affect superhydrophobicity.

To investigate the fundamental processes of wetting under reservoir conditions we have applied a high pressure / high temperature contact angle goniometer (Fig. 7). The instrument has a cylindrical high pressure view cell (HPVC), which can be filled with different fluid or gaseous media. It is possible to study wettability of surfaces and surface tension of different media with the sessile drop and pendant drop method. Experiments can be carried out at realistic reservoir conditions of up to 69 MPa and 180 °C with different fluids and CO_2.

To study the effect of temperature and pressure on the wettability of rough surfaces, a model surface was created that resembles the surface of a lotus leaf (Fig. 8). We used a ceramic aluminum oxide replica of a two-step-photolithographic pillar structure. The sample was coated with a chemically stable, hydrophobic fluorosilane layer. Dynamic contact angle (CA) measurements of water drops in fluid as well as supercritical CO_2 were performed at different temperature and pressure conditions. The pillar surface shows a superhydrophobic behavior with advancing CA of 150-160°, with a slight increase of the CA with pressure (0.1 MPa^{-1}) and a hysteresis of about 15° (Fig. 9). The contact angles at 100 °C show larger slope (0.4 MPa^{-1}) and increased hysteresis (25°) than the data measured at room temperature. The temperature and pressure dependence of the contact angle can be influenced by the interfacial tension of the phases as well as buoyancy effects due to variations of the density.

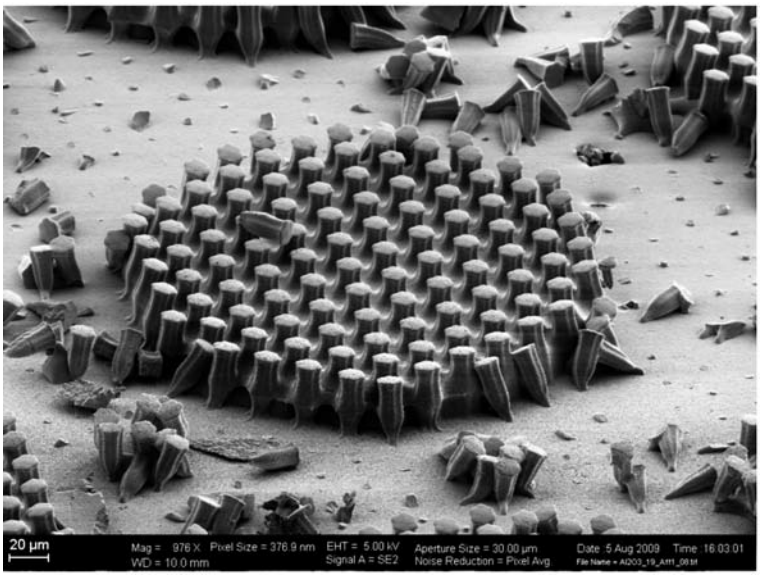

Figure 8: SEM image of a ceramic replica of a pillar structure. The large pillars have a diameter of 100 µm, the small ones 10 µm. The sub-micron scale topography of the sample is dominated by the grain size of the aluminium oxide particles of the slurry used for casting. Due to the undercut shape of the master, part of the small pillars broke off at separation of the replica from the negative (D. Spori, ETH Zurich).

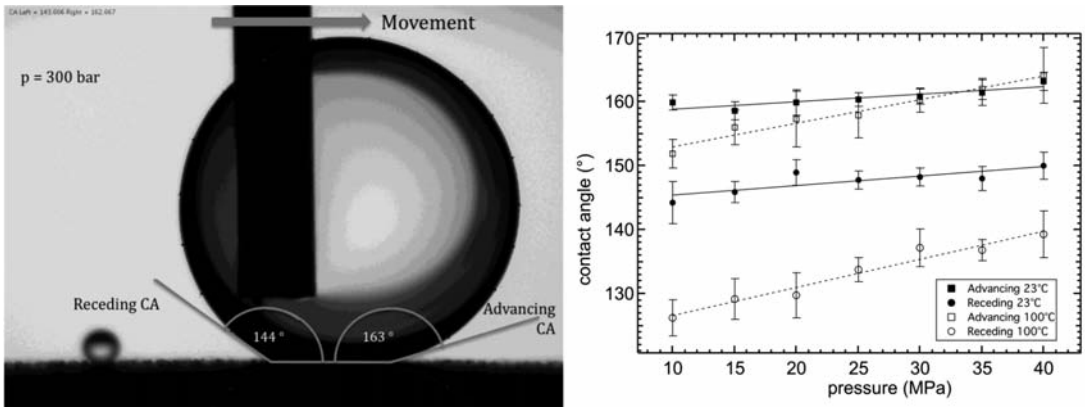

Figure 9: (left) Microphotograph of a water drop on the superhydrophobic pillar structure in liquid CO_2. The surface was moved with respect to the capillary, to measure the advancing and receding contact angle. (right) Contact angles of water in CO_2 at different temperatures and pressures. The data at 100 °C (supercritical CO_2) show a higher slope (0.4°/MPa) and a stronger hysteresis (25°) than the data at room temperature (0.1°/MPa and 15°).

The experiment shows that wetting phenomena caused by surface morphology can also occur under reservoir conditions. Main impact on the details of the wetting (contact angle, hysteresis) can be expected from variations in mass density or surface tension due to mass transfer with the supercritical phase.

Conclusions

The pore space morphology of reservoir rocks depends on the size and shape of the clastic debris and can be drastically changed during diagenesis due to influence of factors such as compaction, cementation, and pressure dissolution. The above observations have led to the conclusions that the pore surfaces at the first phase are rather smooth on a µm scale, and the pores are well-connected facilitating migration of fluids. The subsequent stages of diagenesis, including fluid migration itself, have changed and complicated however, the pore spaces morphology. Pores were filled by minerals and new micro-pores were opened by dissolution of diagenetic minerals. In addition, the grains and cements were partially dissolved, forming new pores within some sedimentary layers or laminae. The overgrowth on clastic grains by secondary minerals produced rough surfaces, leading to more rugged pore surfaces. The flow capacity of hydrocarbon fluids has been decreased due to authigenic

minerals forming barriers and blocking the oil and gas flow. Micro-pore structures and overgrown grain surfaces have formed larger surfaces increasing the adhesion capacity of fluids. Small angle neutron scattering data indicate a mass fractal geometry of the pore space which spans over several orders of magnitude. In the next step the correlation between scattering data (bulk) and the microscopically measured roughness (surface) will be investigated. This correlation provides input for the assessment of the inner roughness of the rock.

The wetting experiments show that the same wetting phenomena (super-hydrophobicity) as known from atmospheric conditions also occur under reservoir conditions. Static and dynamic wetting properties, however, depend on the mass transfer on the phases and thus on the temperature and pressure. Further wetting experiments on model surfaces and on typical minerals like quartz, micas, calcite or feldspars shall provide further insight into the dynamic wetting behavior.

Our research and experiments aim to answer questions imposed by problems occurring in practical oil and gas exploitation activities. It is directed by theoretical petro-physical considerations and practical cases, as discussed with the RWE-Dea, Hamburg, the main oil and gas producer in Germany.

Acknowledgements
We thank the beamline scientists H. Lemmel (TU Wien, Atominstitut) and P. Lindner (ILL Grenoble) for their support in carrying out the neutron scattering experiments. We thank D. Spori and C. Cremmel (ETH Zürich, Laboratory for Surface Science and Technology) for the ceramic replicas.

References

Al-Futaisi, A., Qaboos U, S., Patzek, T.W. and U.C. Berkeley, 2003. Three-phase hydraulic conductances in angular capillaries. SPE J. 8 (3), 252-261.

Al-Futaisi, A., and T.W. Patzek, 2004. Secondary imbibition in NAPL-invaded mixed-wet sediments. J. Contam. Hydrol. 74: 61-81.

Altermann, W., Heckl, W.M., Stark, R.W., Strobel, J. and Ch. Wolkersdorfer, 2008. Nanostructure and wetting properties of sedimentary grains and pore-space surface (NanoPorO). Geotechnologien Science Report No. 12. Koordinierungsbüro Geotechnologien, Potsdam, ISSN 1619-7399, 58-69.

Anovitz, L.M., Lynn, G.W., Cole, D.R., Rother, G., Allard, L..F., Hamilton, W.A., Porcar L. and M.H. Kim, 2009. A new approach to quantification of metamorphism using ultra small and small angle neutron scattering. Geochimica Cosmochimica Acta, 73 (24), 7303-7324.

Barthlott, W. and C. Neinhuis, 1997. Purity of the sacred lotus, or escape from contamination in biological surfaces. Planta. 202, 1-8.

Broseta, D., Barre, L., Vizika, O., Shahidzadeh, N., Guilbaud, J. P. and S. Lyonnard, 2001. Capillary condensation in a fractal porous medium. Phys. Rev. Lett., 86 (23), 5313-5316.

Cassie, A.B.D. and S. Baxter, 1944. Wettability of porous surfaces. Transactions of the Faraday Society. 40: 0546-0550.

Erko, M., Wallacher, D., Brandt, A., and O. Paris, 2010. In-situ small-angle neutron scattering study of pore filling and pore emptying in ordered mesoporous silica. J. Appl. Crystallogr., 43, 1-7.

Fouillac, C., Sanjuan B., Gentier, S., and I. Czernichowski-Lauriol, 2004. Could sequestration of CO2 be combined with the development of enhanced geothermal systems? In: Third Annual Conference on Carbon Capture and Sequestration, Alexandria.

Hassenkam, T., Skovbjerg, L.L., and S.L.S. Stipp, 2009. Probing the intrinsically oil-wet surfaces of pores in north sea chalk at subpore resolution. Proceedings of the National Academy of Sciences (PNAS). 106: 6071-6076.

Jäger, P. and A. Pietsch. 2009. Characterization of reservoir systems at elevated pressure. J. Petrol. Eng. 64, 20-24.

Kremer, B., Bauer, M., Stark, R.W., Gast, N., Altermann, W., Gursky, H-J., Heckl, W.M. and J. Kazmierczak (in press). Raman and atomic force microscopy test for chlorococcalean affinities of problematic Silurian microfossils (»acritarchs«). Journal of Spectroscopy.

Neinhuis, C. and W. Barthlott, 1997. Characterization and distribution of water-repellent, self-cleaning plant surfaces. Annals of Botany. 79: 667-677.

Pape, H., Clauser, C. and J. Iffland, 1999. Permeability prediction based on fractal pore-space geometry. Geophysics, 64 (5), 1447-1460.

Pape, H. and C. Clauser, 2000. Variation of permeability with porosity in sandstone diagenesis interpreted with a fractal pore space model. Pure Appl. Geophys., 157 (4), 603-619.

Pruess, K., 2008. On production behavior of enhanced geothermal systems with CO_2 as working fluid. Energy Conversion and Management. 49, 1446-1454.

Pruess, K. and M. Azaroual, 2006. On the feasibility of using supercritical CO_2 as heat transmission fluid in an engineered hot dry rock geothermal system. In: 31st Workshop on Geothermal Reservoir Engineering, Stanford, CA. SGP-TR-179.

Radlinski, A.P., Ioannidis, M.A., Hinde, A.L. Hainbuchner, M. Baron, M., Rauch, H. and S.R. Kline, 2004. Angstrom-to-millimeter characterization of sedimentary rock microstructure. J. Colloid Interface Sci., 274 (2), 607-612.

Radlinski, A.P., 2006. Small-angle neutron scattering and the microstructure of rocks. Reviews in Mineralogy and Geochemistry, 63, 363-397.

Sen, D. Mazumder, S. and S. Tarafdar, 2002. Pore morphology and pore surface roughning in rocks: A small-angle neutron scattering investigation. J. Mater. Sci., 37 (5), 941-947.

Spori, D.M., T. Drobek, S. Zurcher, M. Ochsner, C. Sprecher, A. Muehlebach, and N.D. Spencer, 2008. Beyond the lotus effect: Roughness, influences on wetting over a wide surface-energy range. Langmuir. 24, 5411-5417.

Sutjiadi-Sia, Y., P. Jaeger and R. Eggers. 2008. Interfacial phenomena of aqueous systems in dense carbon dioxide. J. Supercrit. Fluid., 46, 272-279.

Triolo, F. Triolo, A. Agamalian, M.M. Lin, J.-S. Heenan, R.K. Lucido, G. and R. Triolo, 2000. Fractal approach in petrology: Combining ultra small angle, small angle and intermediate angle neutron scattering. J. Appl. Crystallogr. 33 (1), 863-866.

Wenzel, R.N., 1936. Resistance of solid surfaces to wetting by water. Ind. Eng. Chem. 28, 988-994.

Wong, P.Z. and A.J. Bray, 1988, Porod scattering from fractal surfaces. Phys. Rev. Lett., 60 (13), 1344-1344.

Wong, P.Z. and J. Howard, 1986. Surface roughening and the fractal nature of rocks. Phys. Rev. Lett., 57 (5), 637-640.